Electronic Supplementary Material (ESI) for New Journal of Chemistry.
This journal is © The Royal Society of Chemistry and the Centre National de la Recherche Scientifique 2023

Electronic Supplementary Information

Enhancing the efficiency of benzylamine oxidative coupling over N-doped porous carbon-supported CeO_2 and ZrO_2 nanoparticles

Jie Chen,[a] Mingyuan Jian,[a] Lei Zhuang,[a] Wenting Lin,[a] Yanghe Fu,[a] De–Li Chen,[a] Weidong Zhu[a], Guihua Chen,[b] Fumin Zhang[a]*

[a]Key Laboratory of the Ministry of Education for Advanced Catalysis Materials, Institute of Physical Chemistry, Zhejiang Normal University, Jinhua 321004, People's Republic of China

[b]School of Pharmaceutical and Material Engineering, Taizhou University, 318000 Jiaojiang People's Republic of China

***Corresponding Author:**

Fumin Zhang: zhangfumin@zjnu.edu.cn

1 Experimental

1.1 Chemicals

Zirconium tetrachloride ($ZrCl_4$, 99%) and cerium(III) nitrate hexahydrate (≥99.5%, $Ce(NO_3)_3 \cdot 6H_2O$) were obtained from Meryer Chemical Technology Co., Ltd. 2-aminoterephthalic acid (99.5%), decane (98%), 4-methoxybenzylamine (98%), benzylamine (98%), 2-methylbenzylamine (98%), 3-methylbenzylamine (98%), 4-methylbenzylamine (98%), 4-tert-butylbenzylamine (≥99%), 4-fluorobenzylamine (99%), 4-chlorobenzylamine 99%), 4-bromobenzylamine (99%), aniline (99%), 3-(aminomethyl) pyridine (99%), 2-thiophenemethylamine (99%), 2-furylmethylamine (99%), 4-(trifluoromethyl)benzylamine (99%), dibenzylamine (98%), 1,2,3,4-tetrahydroisoquinoline (95%), N-isopropylbenzylamine (99%) and 1-hexylamine (99%) were purchased from Aladdin Industrial Inc. N, N-dimethylformamide, methanol, ethanol, acetone and acetic acid were supplied by Sinopharm Chemical Reagent Co., Ltd. All chemicals were used without additional purification.

1.2 Characterizations

Powder X–ray diffraction (XRD) patterns were obtained using a D8 Advance powder X–ray diffractometer with Cu Kα radiation (λ = 0.154 nm, operation voltage = 40 kV, operation current = 40 mA) within a 2–theta range of 5° to 80°.

N_2 adsorption–desorption isotherm measurements were conducted using a Micromeritics ASAP 2020 apparatus at 77 K and up to 1 atm. Prior to measurement, samples were degassed under vacuum at 473 K for 15 hours. The specific surface areas in the relative pressure range of P/P_0 = 0.05 to 0.30 were determined using the Brunauer–Emmet–Teller method. Pore size curves were calculated based on the adsorption isotherms using density functional theory, and the micro pore volume was calculated using the *t*–plot method.

Raman spectroscopy was performed using an InVia–Renishaw apparatus and a 532 nm laser source.

Scanning Electron Microscopy (SEM) and Transmission Electron Microscopy (TEM) images were acquired using a Hitachi S–41073 field emission and JEM2100F apparatus at accelerating voltages ranging from 3 to 5 kV and 200 kV, respectively.

Electron Paramagnetic Resonance (EPR) was measured at 298 K under visible light ($\lambda > 420$ nm) conditions using a Bruker EMXplus–9.5/12 spectrometer.

The determination of Ce and Zr metal content in various samples was carried out using Inductively Coupled Plasma Atomic Emission Spectroscopy (ICP–AES) with a Thermo iCAP 7400 instrument. Samples weighing 10 mg were mixed with 3 mL sulfuric acid, 1 mL hydrogen peroxide, and 1 mL hydrofluoric acid in a 50 mL Teflon beaker. The beaker was then covered and heated on a heating plate to 393 K for 12 hours. Once the sample completely dissolved and cooled to room temperature, the resulting solution was transferred to a 50 mL volumetric flask and diluted with deionized water to a total volume of 50 mL.

X–ray photoelectron spectroscopy (XPS) was carried out on a Thermo VG ESCALAB250 with a 300 W Al K radiation. The binding energies were measured with respect to the C1s line of adventitious carbon, which has a reference energy of 284.8 eV, and the base pressure was approximately 3×10^{-9} mbar.

Table S1 Elemental content and textural properties of the various catalysts.

Catalyst	Ce (wt.%)[a]	Zr (wt.%)[a]	S_{BET} (m^2/g)[b]	V_{total} (cm^3/g)[c]	V_{micro} (cm^3/g)[c]
CeZr–NH_2–MOF	0.97	21.98	567.0	0.98	0.13
CeZr–NC–973	1.86	41.82	162.8	0.32	0.00
CeZr–NC–1073	1.96	41.17	189.8	0.34	0.03
CeZr–NC–1173	1.94	43.51	170.9	0.35	0.02

[a]By ICP−AES analysis. [b]By BET method. [c]By *t*−plot method.

Table S2 Cerium and oxygen content in various catalysts analyzed by XPS.

Samples	Ce 3d concentration (%)		O 1s concentration (%)		
	Ce (III)	Ce (IV)	O_{Latt}	O_{Sur}	O_{Ads}
CeZr–NC–973	51.2	48.8	39.3	23.6	37.1
CeZr–NC–1073	57.3	42.7	41.9	46.1	12.0
CeZr–NC–1173	51.0	49.0	48.6	25.4	26.0

Table S3 Optimization of reaction parameters for CeZr–NC–1073 catalyzed oxidative self–coupling of 4–methoxybenzylamine[a].

Entry	T (K)	Solvent	Catalyst amount (mg)	Conv. (%)[b]	Sel. (%)[b]
1	343	*n*–Decane	30	28.5	100
2	363	*n*–Decane	30	44.4	100
3	383	*n*–Decane	30	97.1	100
4	383	Dodecane	30	80.3	100
5	383	EtOH	30	21.7	67.8
6	383	Acetonitrile	30	34.2	100
7	373	H_2O	30	3.9	28.1
8	383	DMF	30	99.2	35.3
9	383	Toluene	30	64.9	100
10	383	Paraxylene	30	42.0	100
11	383	*n*–Decane	15	36.3	100
12	383	*n*–Decane	25	65.3	100
13	383	*n*–Decane	35	97.2	88.0
14[c]	383	*n*–Decane	30	64.9	67.8
15[d]	383	*n*–Decane	30	74.2	74.5

[a]**Reaction conditions**: 4–Methoxybenzylamine (0.5 mmol), solvent (3 mL), O_2 (1 atm), 8 h. [b]Determined by gas chromatography using diphenyl as the internal standard. [c]Under an air atmosphere. [d]Under a N_2 atmosphere.

Table S4 Comparison of catalytic oxidative coupling of benzylamine over different catalysts.

Entry	Catalyst	Reaction conditions Substrate/catalyst-dosage/temperature/oxidant	Con. (%)	Sel. (%)	Ref.
1	CeZr–NC–1073	0.5 mmol/30 mg/383 K/1 atm O_2/8 h	99.5	100.0	This work
2	CeO_2–MoO_3/SiO_2	1 mL·h^{-1}/300 mg/493 K/60 mL·min^{-1} O_2/6 h	96.0	97.8	[s1]
3	MoO_x/CeO_2–ZrO_2	0.2 mmol/100 mg/383 K/20 mL·min^{-1} O_2/6 h	99.0	99.8	[s2]
4	$Ce_{0.95}Cu_{0.05}O_2$–300	3 mmol/50 mg/383 K/1 atm air (0.3 mmol NHPI)/48 h	97.8	98.6	[s3]
5	$Ce_{0.8}Eu_{0.2}O_{2-\delta}$/$SiO_2$	0.2 mmol/100 mg/398 K/20 mL·min^{-1} O_2/7 h	99.0	99.8	[s4]
6	Au–CeO_2–ZrO_2	0.2 mmol/100 mg/403 K/20 mL·min^{-1} O_2/6 h	95.0	99.9	[s5]
7	CeMn-RO	2 mmol/50 mg/353 K/1 atm air/8 h	92.0	80.0	[s6]
8	α–MnO_2	0.5 mmol/10 mol%/RT/1 mmol TBHP/4 h	99.0	95.0	[s7]
9	NHPI/Fe(BTC)	0.5 mL/75 mg/373 K/1 atm O_2/24 h	98.0	90.0	[s8]

Reference

[s1] B. G. Rao, P. Sudarsanam, B. Mallesham and B. M. Reddy, *RSC Adv.*, 2016, **6**, 95252–95262.

[s2] A. Rangaswamy, P. Sudarsanam, B. G. Rao and B. M. Reddy, *Res. Chem. Intermed.*, 2015, **42**, 4937–4950.

[s3] X. Huang, G. Lu, K. Zhang, J. Liu, H. Zhang, Z. Guo and J. Tao, *Appl. Surf. Sci.*, 2020, **514**, 145948.

[s4] T. Vinodkumar, J. K. P. Kumar and B. M. Reddy, *J. Chem. Sci.*, 2021, **133**, 68.

[s5] P. Sudarsanam, B. Mallesham, A. Rangaswamy, B. G. Rao, S. K. Bhargava and B. M. Reddy, *J. Mol. Catal. A: Chem.*, 2016, **412**, 47–55.

[s6] C. Wu, J. Bu, W. Wang, H. Shen, Y. Cao and H. Zhang, *Ind. Eng. Chem. Res.,* 2022, **61**, 5442–5452.

[s7] Z. Zhang, F. Wang, M. Wang, S. Xu, H. Chen, C. Zhang and J. Xu, *Green Chem.*, 2014, **16**, 2523–2527.

[s8] A. Dhakshinamoorthy, M. Alvaro and H. Garcia, *ChemCatChem*, 2010, **2**, 1438–1443.

Table S5 Kinetic parameters of the CeZr–NC–1073 catalyzed oxidative self–coupling reaction of 4–methoxybenzylamine.

T (K)	k (min^{-1})	E_a (kJ/mol)
363	2.5×10^{-3}	
373	4.1×10^{-3}	62.6 ± 3.0
383	7.3×10^{-3}	

Table S6 Effect of scavenger agent on oxidation of 4–methoxybenzylamine to imine in the presence of CeZr–NC–1073[a].

Entry	Scavenger	Conv. (%)[b]	Sel. (%)[b]
1	Blank	97.8	100
2	benzoquinone	96.8	100
3	BHT	38.4	100
4	TEMPO	75.9	92.0
5[c]	Blank	58.0	100
6[d]	Blank	55.4	100
7[e]	Blank	53.7	100

[a]**Reaction conditions**: 4–Methoxybenzylamine (0.5 mmol), catalyst (30 mg), *n*–decane (3 mL), O_2 (1 atm), 383 K, 8 h. [b]Determined by gas chromatography using diphenyl as the internal standard. [c]2 h. [d]In the presence of 3 Å molecular sieve (0.15 g). [e]With adding H_2O (1 mmol).

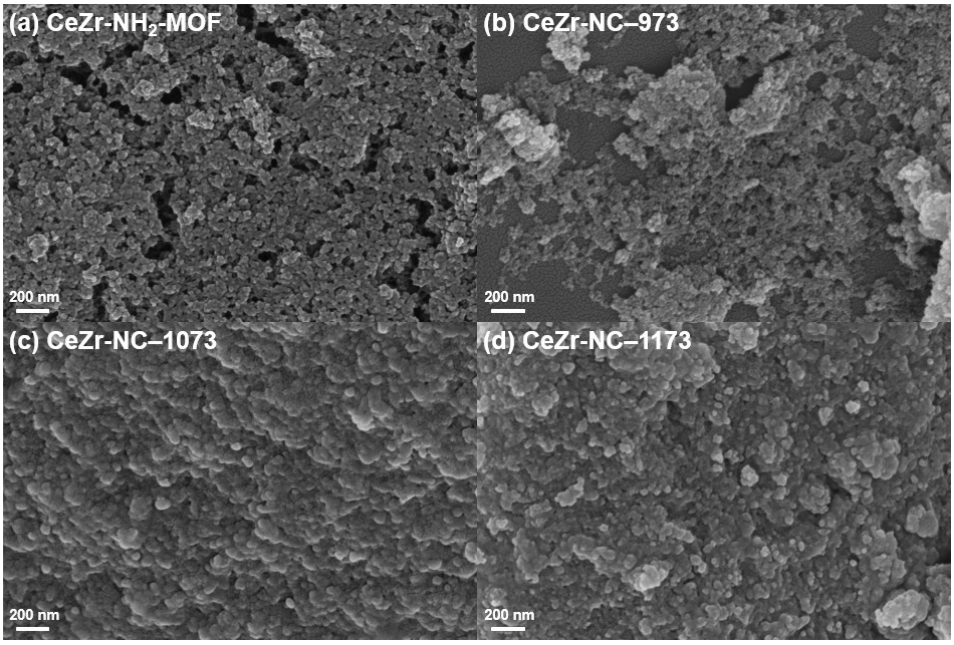

Figure S1 SEM images of (a) CeZr–NH_2–MOF, (b) CeZr–NC–973 (c) CeZr–NC–1073 and (d) CeZr–NC–1173.

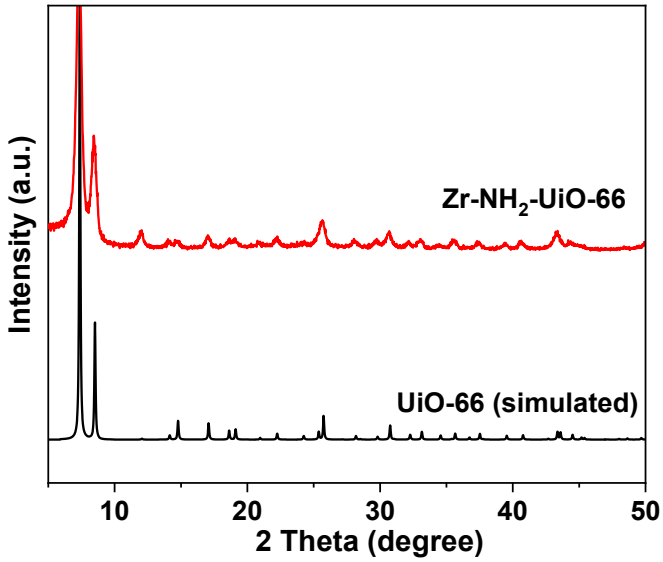

Figure S2 XRD pattern of Zr–NH_2–UiO–66.

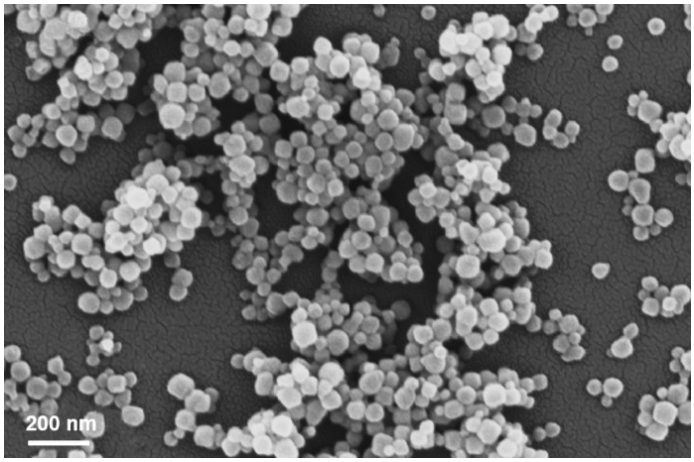

Figure S3 SEM image of Zr–NH_2–UiO–66.

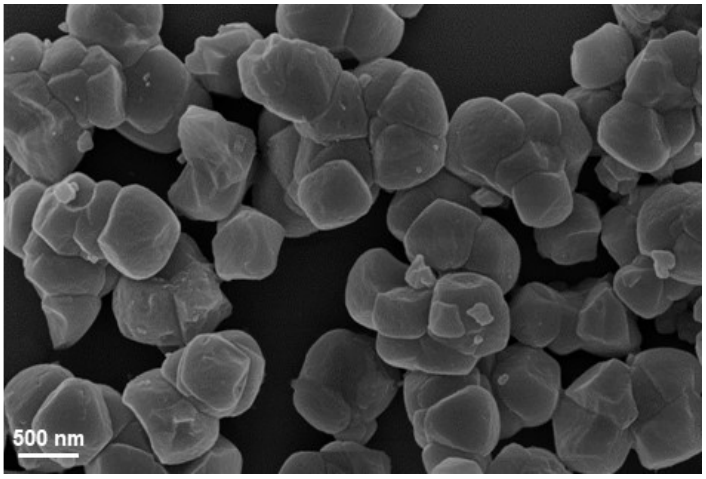

Figure S4 SEM image of Ce–UiO–66.

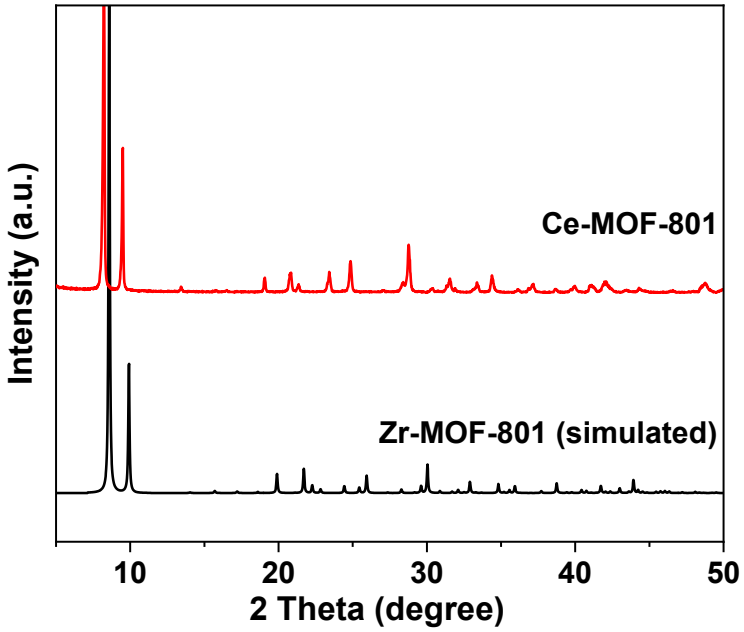

Figure S5 XRD pattern of Ce–MOF–801.

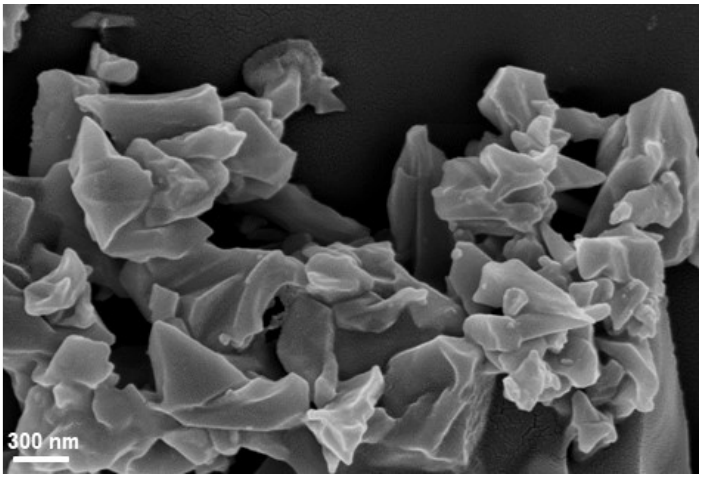

Figure S6 SEM image of Ce–MOF–801.

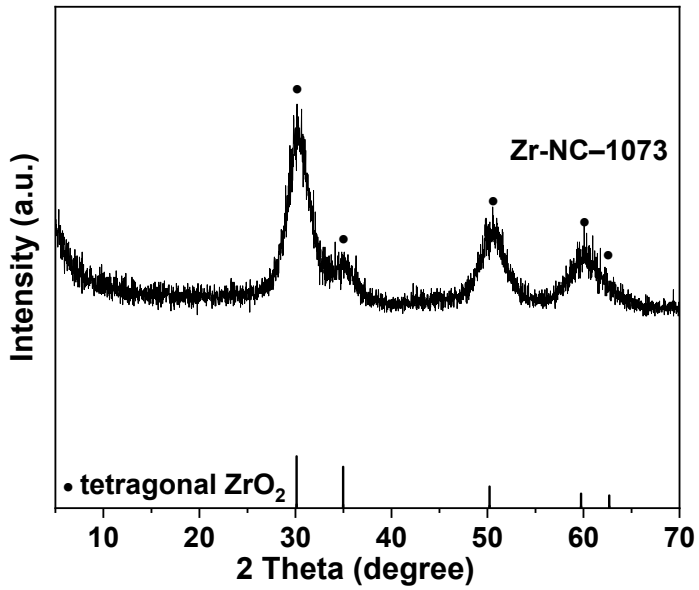

Figure S7 XRD pattern of Zr–NC–1073.

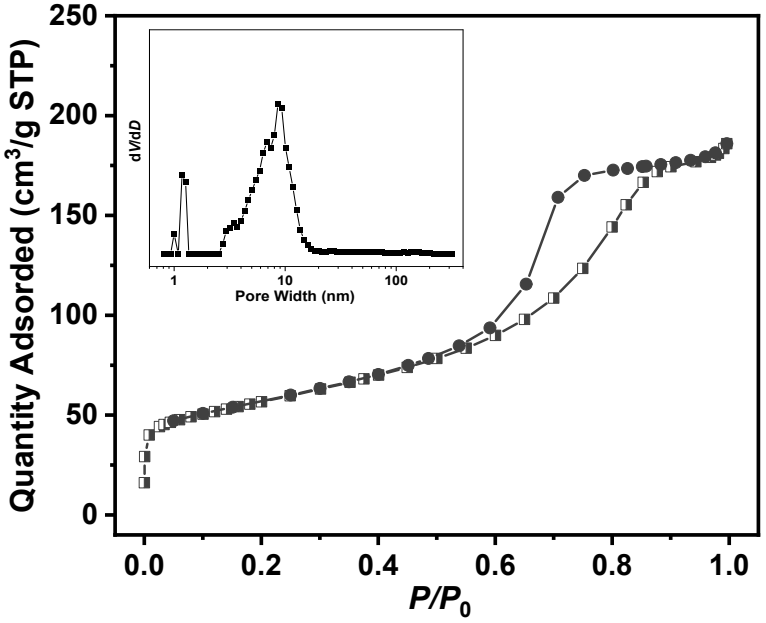

Figure S8 N_2 adsorption–desorption isotherms and the corresponding pore size distribution of Zr–NC–1073.

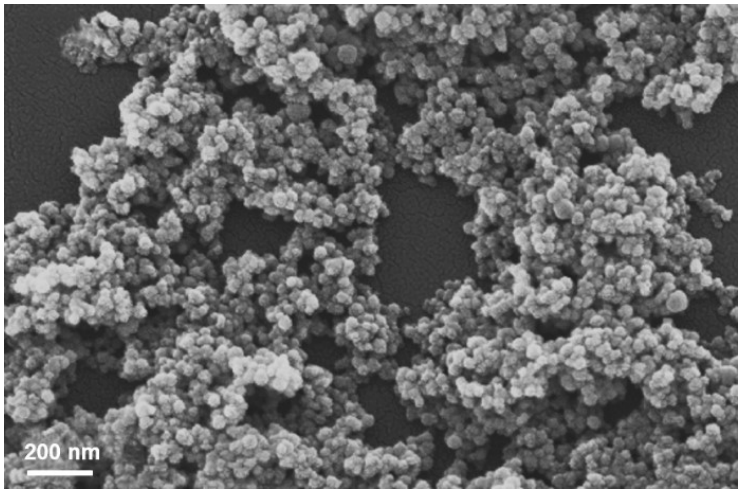

Figure S9 SEM image of Zr–NC–1073.

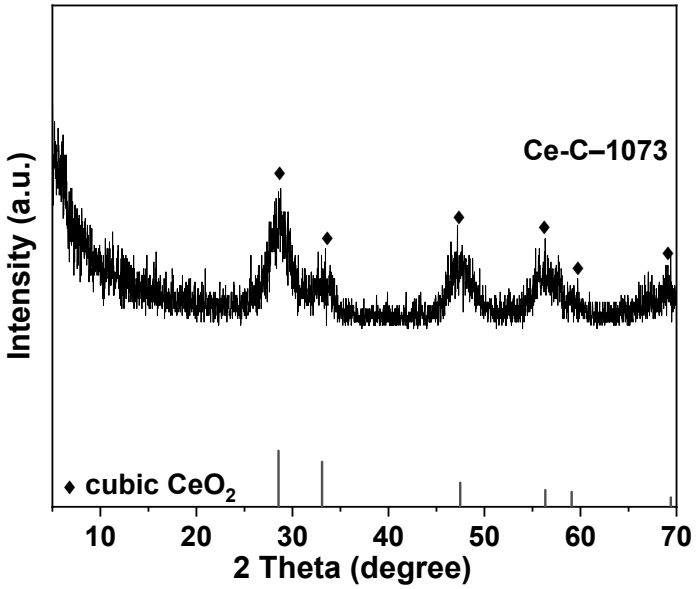

Figure S10 XRD pattern of Ce–C–1073.

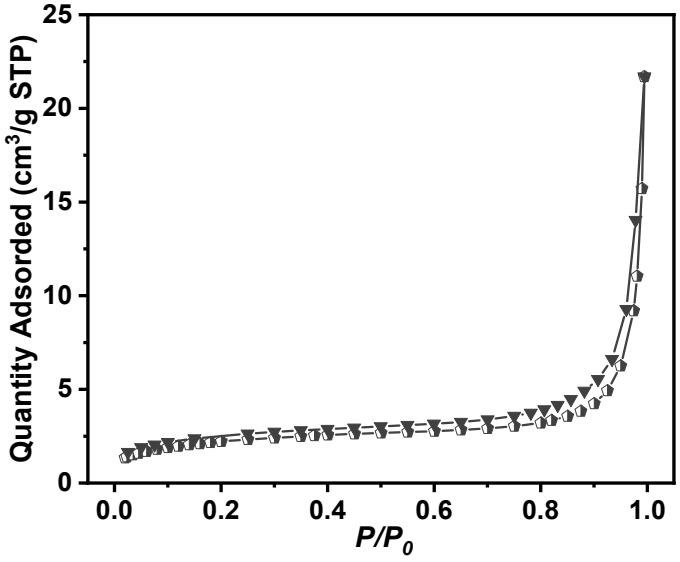

Figure S11 N_2 adsorption–desorption isotherms of Ce–C–1073.

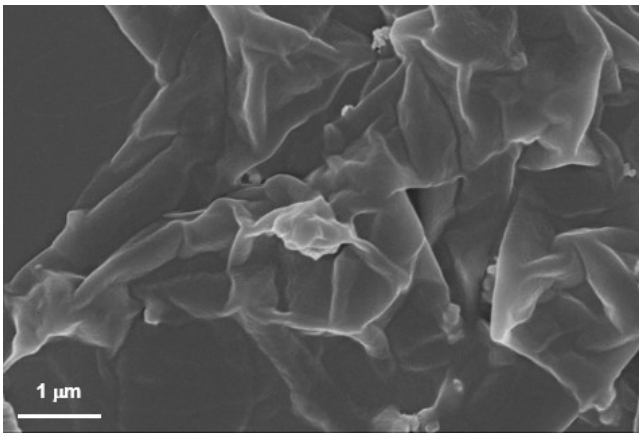

Figure S12 SEM image of Ce–C–1073.

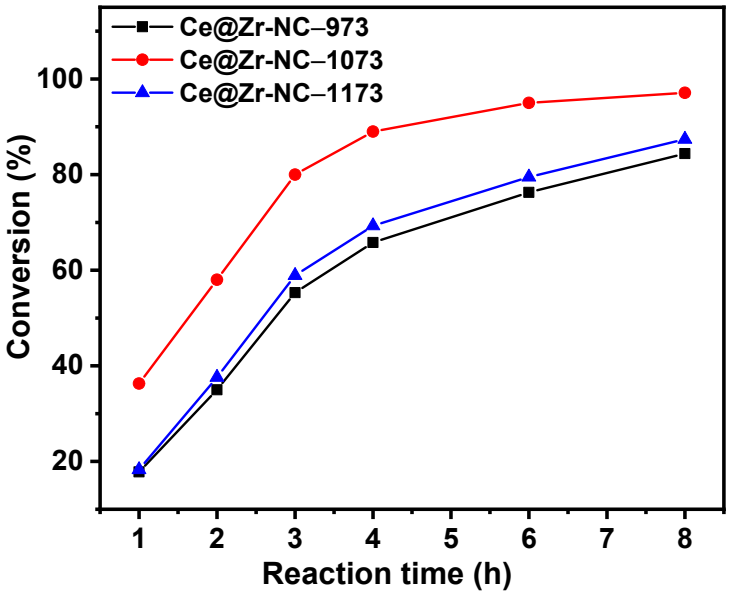

Figure S13 Plot of conversion versus reaction time over CeZr–NC–T. Reaction conditions: 4–methoxybenzylamine (0.5 mmol), CeZr–NC–T (30 mg), *n*–decane (3 mL), O_2 (1 atm), 383 K.

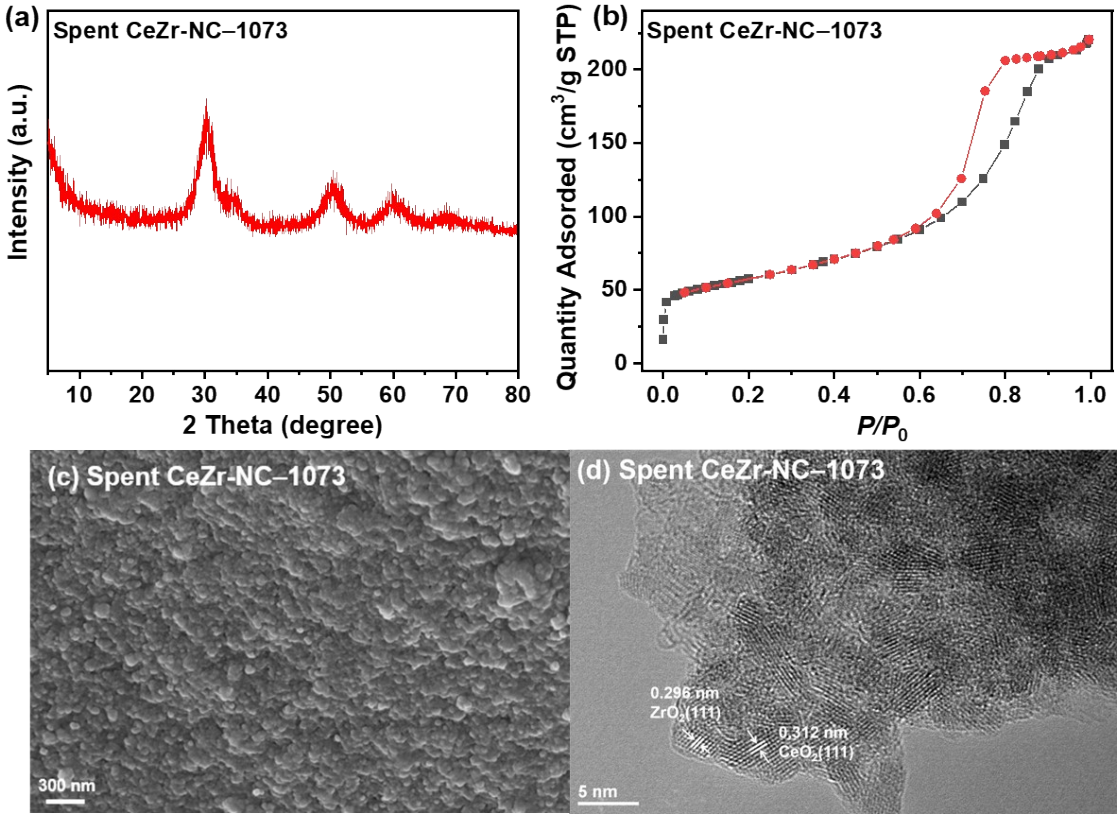

Figure S14 (a) XRD pattern, (b) N_2 adsorption–desorption isotherms, (c) SEM, and (d) TEM of spent CeZr–NC–1073.

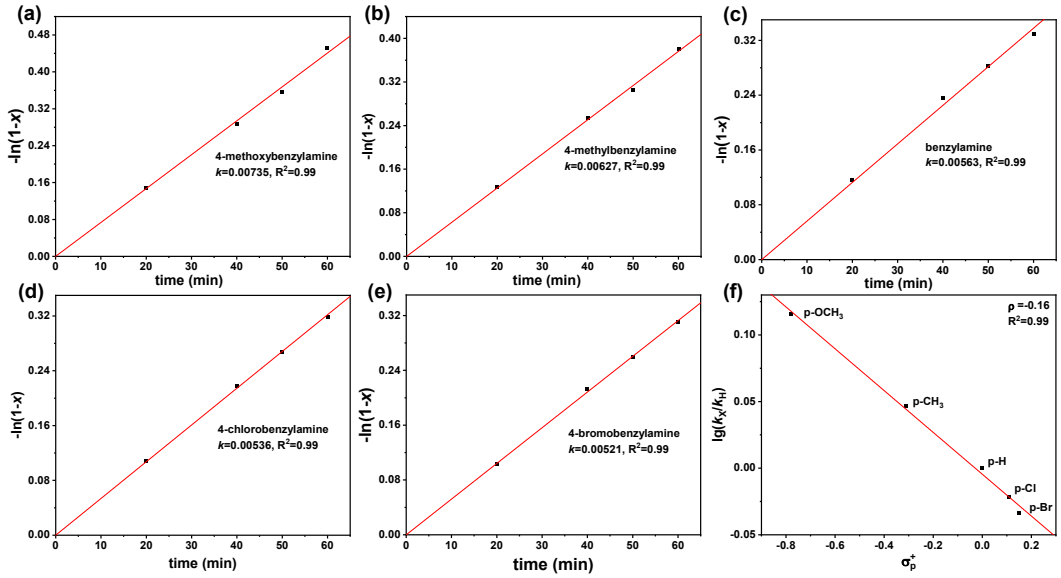

Figure S15 (a)~(e) Plot of –ln(1–x) versus reaction time for five substituted benzylamines. (f) Hammett plot for the self–coupling of *p*–substituted benzylamines over CeZr–NC–1073, and the lg(k_x/k_H) was obtained from the ratio of the conversion with a reaction time of 1 h. σ^+ is the Brown−Okamoto constant. **Reaction conditions**: substituted benzylamines (0.5 mmol), CeZr–NC–1073 (30 mg), *n*–decane (3 mL), O_2 (1 atm), 383 K.